Measurement of the ^{209}Bi(n,4n)^{206}Bi and ^{169}Tm(n,3n)^{167}Tm cross sections between 23.5 and 30.5 MeV relevant to reaction-in-flight neutron studies at the National Ignition Facility

M. E. Gooden, T. A. Bredeweg, B. Champine, D. C. Combs, S. Finch, A. Hayes-Sterbenz, E. Henry, Krishichayan, R. Rundberg, W. Tornow, J. Wilhelmy, and C. Yeamans

Phys. Rev. C **96**, 024622 — Published 28 August 2017

DOI: 10.1103/PhysRevC.96.024622

Measurement of the ^{209}Bi(n,4n)^{206}Bi and ^{169}Tm(n,3n)^{167}Tm Cross Section Between 23.5 and 30.5 MeV Relevant To Reaction-In-Flight Neutron Studies at the National Ignition Facility

M.E. Gooden,[1,*] T.A. Bredeweg,[1] B. Champine,[2] D.C. Combs,[3,4] S. Finch,[5,4] A. Hayes-Sterbenz,[1] E. Henry,[6] Krishichayan,[5,4] R. Rundberg,[1] W. Tornow,[5,4] J. Wilhelmy,[1] and C. Yeamans[6]

[1] *Los Alamos National Laboratory, Los Alamos, NM 87545*
[2] *University of California Berkeley, Berkeley, CA 94720*
[3] *North Carolina State University, Raleigh, NC 27695*
[4] *Triangle Universities Nuclear Laboratory, Durham, NC 27705*
[5] *Duke University, Durham, NC 27705*
[6] *Lawrence Livermore National Laboratory, Livermore, CA 94550*

(Dated: August 7, 2017)

At the National Ignition Facility experiments are being performed to measure charged-particle stopping powers in the previously unexplored warm dense plasma regime. These measurements are done using reaction-in-flight (RIF) neutrons from an inertial confinement fusion system. RIF neutrons are produced with a continuum of energies up to 30 MeV. By making activation measurements utilizing threshold reactions for neutrons in the energy range of $15 < E_n < 30$ MeV, the number of RIF neutrons can be determined and from this the stopping power of the deuterium and tritium ions that produced the RIF neutrons can be inferred. Currently, the ^{169}Tm(n,3n)^{167}Tm reaction has been used. However, in an effort to provide a secondary complimentary measurement, efforts are underway to make us of the ^{209}Bi(n,4n)^{206}Bi, with a threshold of 22.5 MeV. The cross-sections were measured at the 10 MV Tandem Van De Graaff at the Triangle Universities Nuclear Laboratory with quasi-monoenergetic neutrons between 23.5 - 30.5 MeV, where few previous measurements have been made. Cross-section data are compared to calculations and other available measurements.

I. INTRODUCTION

Inertial Confinement Fusion (ICF) experiments on the National Ignition Facility (NIF) at Lawrence Livermore National Laboratory (LLNL) provide a unique platform for a number of nuclear and plasma physics measurements [1]. The HighFoot campaign at NIF has achieved some of the highest areal-density (ρR) with cryogenic targets, which has allowed the novel study of charged-particle stopping powers in warm dense plasma to be done for the first time. These measurements are accomplished with neutron activation techniques using various thresholding reactions to measure Reaction-In-Flight (RIF) neutrons produced in the compressed cryogenic capsule. RIF neutrons are produced when an initial 14.1 MeV neutron from a pair of fusing D-T (denoting ^{2}H and ^{3}H, respectively) ions up-scatters a D or T ion before it undergoes a separate D-T fusion reaction. These RIF neutrons are produced in a continuum up to $\sim$30 MeV and are responsible for nearly all the neutrons above the 14 MeV fusion peak as shown in Fig. 1 [2]. Since the production of the RIF neutrons requires a neutron to scatter off of a D or T ion, there must be a sufficiently high density of D or T ions and neutron. In HIghFoot shots, the highest density of D and T ions occurs in the cryogenic ice layer on the inner walls of the capsule. It is, therefore, in this region where there is the highest probability of up-scattering D or T ions and thus is the region where dominate yield of RIF neutrons are produced. It is the plasma conditions of this ice layer which are of interest, and in which the stopping power is measured through measurement of the RIF neutron spectrum. The RIF neutrons contribute only 10^{-4} to the total neutron yield, and therefore, are difficult to measure in the presence of the strong 14.1 MeV fluence. Presently, the ^{169}Tm(n,3n)^{167}Tm reaction has been used to measure the RIF neutrons above its 14.9 MeV threshold, leading to new data on stopping power models [2]. It is clear from [2] that the cross section of the reaction is a necessary component in determining the stopping powers and therefore, the relevant nuclear data must be measured to fully interpret the results. In support of the RIF measurements, the ^{169}Tm(n,3n)^{167}Tm cross-section has been recently measured [3]. As an additional measurement of the RIF neutron spectrum, the ^{209}Bi(n,4n)^{206}Bi reaction is now being employed, with a threshold of 22.5 MeV. This reaction serves the dual purposes of providing a secondary measurement to complement the Thulium studies and also provides new insight on the stopping power of higher energy up-scattered charged particles.. The ^{209}Bi(n,4n)^{206}Bi reaction is used for high incident neutron energies (up to 100's of MeV) for dosimetry in accelerator applications: isotope production, transmutation of waste, etc. [4]. Therefore, in the energy range of interest between 22.5 - 30 MeV, only a few measurements of this cross-section exists ([4, 5]). We have therefore measured this cross-section in approximately 1 MeV steps over the energy range of interest to the RIF program at NIF. In addition, we report new results on new measurements of the ^{169}Tm(n,3n)^{167}Tm reaction in this

* m_gooden@lanl.gov

same 22.5-30 MeV neutron energy range.

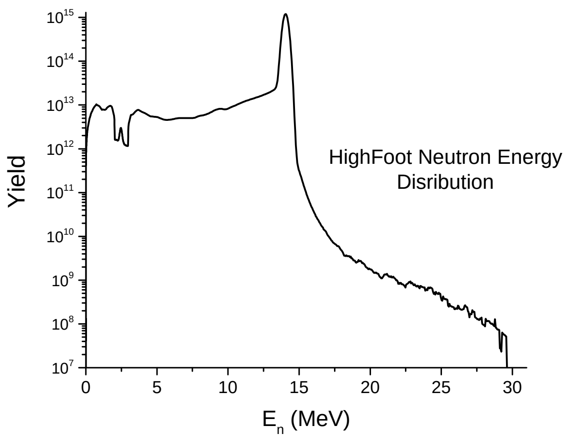

FIG. 1. Simulated neutron spectrum from a HighFoot implosion on the NIF.

II. EXPERIMENT

The measurements of the ^{209}Bi(n,4n)^{206}Bi cross-section were performed using the 10 MV FN Tandem Van De Graaff Accelerator at the Triangle Universities Nuclear Laboratory (TUNL) on the campus of Duke University. Quasi-monoenergetic neutrons were produced with the ^{3}H(d,n)^{4}He reaction, the same hydrogen fusion reaction employed at NIF. Accelerated deuterons were incident onto a neutron production target consisting of 2.1 Ci Tritium absorbed onto a 19 mm diameter deposit of Titanium on a 0.4 mm thick Cu backing, giving a ratio of T/Ti of >1.5. Approximately 1.5 atmospheres of He gas was used between a 6.5 μm Havar foil separating the accelerator vacuum and the Ti-T target to help with cooling the tritiated target. A schematic of the gas-cell/Ti-T neutron production target is given in Fig. 2.

The ^{209}Bi(n,4n)^{206}Bi and ^{169}Tm(n,3n)^{167}Tm reaction cross-sections were measured at eight incident neutron energies: 23.5, 24.9, 25.5, 26.5, 27.5, 28.5, 29.5 and 30.5 MeV. The neutron flux was determined using the ^{209}Bi(n,3n)^{207}Bi reaction as a reference reaction. This has the advantage that the flux is measured simultaneously in the same location as the main reaction of interest (^{209}Bi(n,4n)). The Bismuth targets were 0.9525 mm in diameter and 1 mm thick, while the Thulium foils were the same diameter but 0.1 mm thick. The foils were stacked (Tm/Bi) and placed ∼16 mm from the outer flange of the gas-cell assembly, with the Thulium foil nearest the neutron production target. This gives a distance of ∼18 mm from the tritiated target to the foil stack. This distance was used to maximize neutron flux while attempting to minimize the neutron energy spread due to the angular distribution of the ^{3}H(d,n)^{4}He reaction [6].

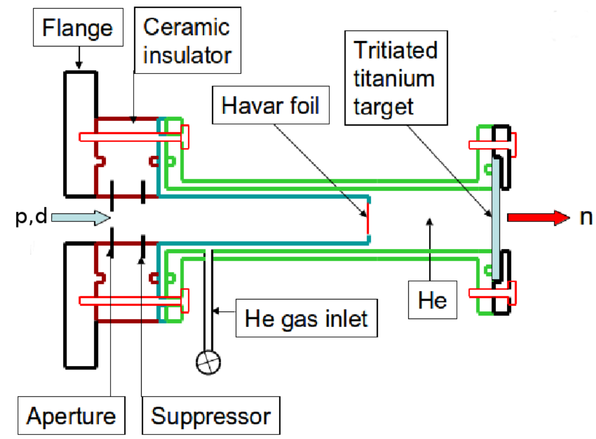

FIG. 2. (Color online) Schematic of gas-cell and tritiated target assembly for neutron product at TUNL.

TABLE I. Information on foils used and each incident neutron energy. Spread in neutron energy is corrected for the broadening due to detector resolution. Uncertainty in the foil masses is ±1E-4 g.

Energy (MeV)	Bi Mass (g)	Tm Mass (g)
23.5 ± 0.105	0.7393	0.0681
24.9 ± 0.130	0.7436	0.0680
25.6 ± 0.133	0.7355	0.0670
26.5 ± 0.138	0.7416	0.0684
27.5 ± 0.142	0.7386	0.0688
28.5 ± 0.147	0.7393	0.0683
29.5 ± 0.156	0.6833	0.0695
30.5 ± 0.165	0.6833	0.0684

Each foil stack was irradiated for between 24-72 hours depending on the calculated ^{209}Bi(n,4n)^{206}Bi cross-section and the known cross-section of the reference reaction. After the irradiation, the foils were mounted in front of lead shielded High-Purity Germanium (HPGe) detectors for gamma-ray counting for ∼24 hours. The Bismuth foils were counted at 2.5 cm from the face of one HPGe detector, while the Tm was counted at 5 cm on a separate, but nearly identical, HPGe detector. At the lowest neutron energies the count rates for the Tm foils were sufficient to allow counting at both 5 cm and a well calibrated further position, typically 15 cm. Similarly, the Bi foils could be counted at far geometries for the higher energy bombardments where the production yields were larger. This allowed for precise calibration of the geometry (foil diameter/thickness, etc.) for the specific gamma-rays of each foil. Using this approach, the overall photopeak detection efficiencies were determined to a range of 1-1.5%, see Table III, while automatically including such effects as attenuation and coincidence-summing. Due to the long half-life of the reference reaction used (31.55 years), the Bismuth samples were returned to LANL and counted on the Compton suppressed dual-clover HPGe detector system [2], that has significantly higher efficiency than the other HPGe detectors.

At each neutron energy, a neutron time-of-flight (NTOF) was taken by pulsing the incident deuteron beam at a frequency of 2.5 MHz (2-3 ns wide pulse), using the pulsing and bunching system at TUNL. The NTOF measurements were made with a BC-501A neutron scintillation detector at 360 cm from the neutron production target. The various NTOF measurements are shown together in Fig. 3, where each measurement has been normalized to the area of the prompt neutron peak of the ^{3}H(d,n)^{4}He reaction. There is an $\sim$10 MeV 'clean' region between the prompt or on-energy neutrons and low-energy neutrons from various other neutron production and deuteron breakup reactions. The broadness of the prompt neutron peak is due to the timing of the neutron detector and is in reality much smaller. The incident energies and their associated spread are given in Table I, along with the masses of the Bismuth and Thulium targets used at each energy.

The neutron energy distribution for the neutrons of interest was calculated based on the width of the neutron beam as determined by the NTOF once the detector resolution is unfolded and also included the ^{3}H(d,n)^{4}He neutron angular distribution over the foil geometries weighted by the cross-section [3]. This calculation produces a neutron energy distribution for each incident neutron energy similar to the one in Fig. 4. The effect of the angular distribution is to broaden and slightly lower the average neutron energy versus that seen in the NTOF.

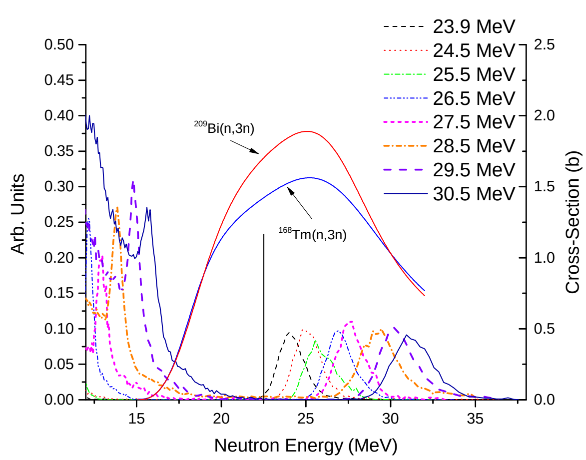

FIG. 3. (Color Online) Evaluated cross-section data used for flux determination from reference reactions overlaid with the neutron Time-of-Flight spectra normalized for comparison. TOF spectra shown are uncorrected for neutron detector efficiency or resolution. The vertical line is the location of the ^{209}Bi(n,4n)^{206}Bi reaction threshold.

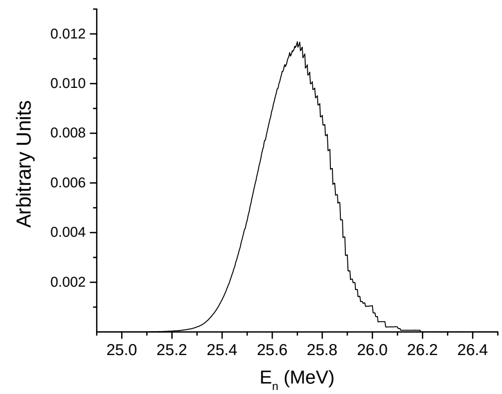

FIG. 4. Calculated neutron energy distribution using the cross-sections and angular distribution of the ^{3}H(d,n)^{4}He reaction [6] averaged over the geometry of the measurement.

The most comprehensive set of cross-sections for the neutron flux monitor reference reactions was found from Zolotarev in the IRDFF evaluation [7]. These evaluations were chosen over the ENDF/B-VII.1 [8] as they extended above 20 MeV and provide uncertainties for each point. The evaluated cross-sections for the ^{209}Bi(n,3n)^{206}Bi and ^{169}Tm(n,3n)^{167}Tm reactions are shown in Fig. 3. The Thulium cross-section evaluation is necessary to make corrections for off-energy neutrons. Eq. 1 [9] is used to determine the cross-section of interest. The flux is determined using the same equation rearranged with the flux ϕ on the left, since the reference cross-section is know [10–12].

$$\sigma = \frac{N_\gamma \lambda C_1 C_2}{\phi N_a I_\gamma \epsilon_\gamma e^{-\lambda t_d}(1-e^{-\lambda t_{irr}})(1-e^{-\lambda t_c})}. \quad (1)$$

In Eq. 1, N_γ is the photo-peak yield from γ-ray counting, N_a is the number of atoms in the foil of interest, I_γ and ϵ_γ are the γ-ray emission probability and counting efficiency respectively. The times t_d, t_{irr} and t_c are: the decay time from end of irradiation to beginning of counting, the irradiation length and the γ-ray counting length, respectively. The correction factor C_1 corrects for fluctuations in the neutron intensity during the irradiation using sampling of the beam current from a beam-current integrator recorded every 8 seconds throughout the run [9]. This correction is very small, i.e. nearly equal to 1.00.

$$C_2 = 1 - \frac{\int_0^{E_c} \phi(E)\sigma(E)dE}{\int_0^{E_c} \phi(E)\sigma(E)dE + \phi_x\sigma_x}. \quad (2)$$

The factor C_2 is a correction that deals with the off-energy neutrons that are above the reaction thresholds of the reference reaction as well as the ^{169}Tm(n,3n)^{167}Tm reaction. The off-energy neutrons are below the threshold of the ^{209}Bi(n,4n)^{206}Bi reaction as shown in Fig. 3.

Since these off-energy neutrons contribute to the reference reaction they must be corrected for to properly determine the neutron flux for only the on-energy neutrons of interest. C_2 is determined by Eq. 2 and the value of this correction and its uncertainty is given in Table II. The flux $\phi(E)$ is determined from the measured NTOF spectra corrected for the efficiency of the neutron detector. From Fig. 3 it is clear that for the majority of the energies, the off-energy neutron spectra samples only a small portion of the reference reaction cross-sections, as is confirmed by the correction factors in Table II.

Shown in Table III is a breakdown of the uncertainties for the different components of the measurements. As shown, the largest source of uncertainty is in the uncertainty of the reference ^{209}Bi(n,3n)^{207}Bi reaction used to determine the neutron flux. As discussed above, where possible, the samples were counted at both a close and far geometry. This approach establish an accurate procedure for establishing the efficiencies of the high geometry locations and allows higher precision in determining the reaction cross sections nearer to threshold where yields are low. The 3.8% uncertainty in the γ-ray emission probability for the 207 keV transition in the decay of ^{167}Tm is taken from a recent measurement by Champine et. al. [3].

III. RESULTS AND DISCUSSION

A. ^{209}Bi(n,4n)

These measurements represent the most complete set of data for the ^{209}Bi(n,4n)^{206}Bi reaction from threshold to 30 MeV. The results are given in Table IV and Figs. 5 and 6. There exists only a limited number of previous data sets for this reaction, and in the energy range of interest only a handful of data points have been measured. Fig. 5 presents the results obtain in this series of measurements along with existing data up to 50 MeV, as well as evaluations from the TALYS Evaluated Nuclear Data Library (TENDL) [13] and the European Activation File (EAF) [14].

The literature data in Fig. 5 were all produced with the p-Li reaction, resulting in a much larger energy spread and off-energy neutron contribution than obtained with the ^{3}H(d,n)^{4}He reaction used here; this is seen by the data shown in Fig. 6. Overall there is good agreement between the present data and the other measured data. The Zaman data [15] at 26.5 MeV samples a large portion of the cross-section due to its wide energy resolution, this probably contributes to it being high compared to the present data at the same energy that has a resolution ~ 20x better.

The 27.6 MeV Kim data [5] is 15% higher than the present value at 27.4 MeV, but neglecting the 200 keV energy difference the two values are consistent within uncertainties. At ~29.5 MeV the recently published result by Majerle et al. [16], is low compared with the present data by a factor of ~1.4, however, their lowest energy point (24.5 MeV) agrees nicely with the present data at 23.9 and 24.9 MeV. In Fig. 5, the lowest three data points from Vrzalova [4], up to 50 MeV are shown, the only point that overlaps with the present energy range of interest is at 30.5 MeV and is within 1.5% of the present work.

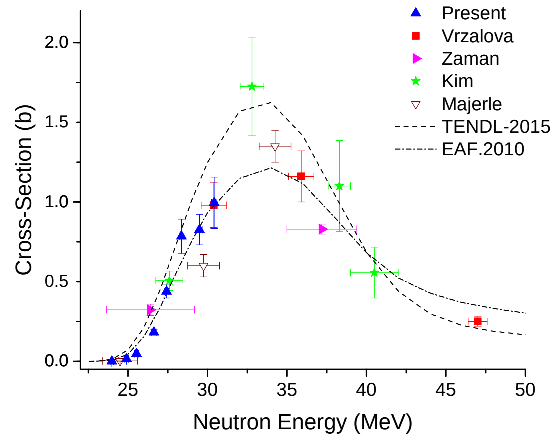

FIG. 5. (Color Online) Present data for the ^{209}Bi(n,4n)^{206}Bi reaction, along with existing experimental data up to 50 MeV.

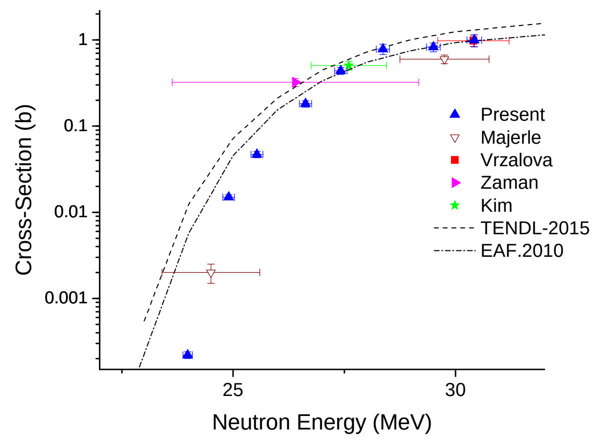

FIG. 6. (Color Online) Present data for the ^{209}Bi(n,4n)^{206}Bi reaction, along with existing experimental data up to 32 MeV in log-scale for comparison.

The present data and existing literature data agree reasonably well between ~26-30 MeV, with the TENDL-2015 and EAF-2010 evaluations. It is clear that TENDL is tied to the Kim data, while EAF, gives preference to the Vrzalova values, see Fig. 5. Below, 26 MeV, the present data agrees with the EAF evaluation much better than TENDL, possibly a result of the Kim data at ~32 MeV. However, both evaluations predict a much larger cross-section above threshold than was measured. No evaluation for this reaction was found from ENDF/B-

TABLE II. Off-energy neutron correction, C_2, to the reference reactions used to determine the neutron flux.

Foil	Energy (MeV) 23.9	24.9	25.6	26.5	27.5	28.5	29.5	30.5
^{209}Bi(n,3n)^{207}Bi	0.9993(1)	0.9986(1)	0.9991(1)	0.9888(8)	0.9380(41)	0.899(11)	0.788(24)	0.533(75)
^{169}Tm(n,3n)^{167}Tm	0.9994(1)	0.9988(1)	0.9993(1)	0.9890(9)	0.9450(45)	0.886(13)	0.809(25)	0.629(52)

TABLE III. Breakdown of sources of uncertainties and their magnitudes at the 1σ level. See text for details.

Source of Uncertainty	Magnitude (%)
Target Masses	$\ll$0.02
Photo-Peak Area	0.1-3.5
γ-ray Efficiency	1.19-1.42
Neutron Intensity Fluctuation	0.1
Neutron Monitor Efficiency	3-5
γ-ray Emission Probability	0.1-3.8
Flux Monitor X-sections	5-12

TABLE IV. Results from present measurements for the ^{209}Bi(n,4n)^{206}Bi reaction with quasi-monoenergetic neutrons. Uncertainties are given at the 1σ level.

Energy (MeV)	σ (b)
23.9 ± 0.105	2.2E-4 ± 2E-5
24.9 ± 0.130	0.015 ± 0.001
25.5 ± 0.133	0.047 ± 0.004
26.5 ± 0.138	0.182 ± 0.016
27.5 ± 0.142	0.438 ± 0.041
28.5 ± 0.147	0.785 ± 0.107
29.5 ± 0.156	0.826 ± 0.095
30.5 ± 0.165	0.995 ± 0.162

VII.1 [8], or other major libraries.

B. ^{169}Tm(n,3n)

The cross-section results for the ^{169}Tm(n,3n)^{167}Tm reaction are shown in Table V and Fig. 7. The most complete set of measurements for this reaction come from Bayhurst [17]. The lowest three data points from the present results agree within uncertainties with the existing data. However, the data at 26.5, 27.5 and 28.5 MeV are higher than Bayhurst or Uno [18]; ∼20% for the data at 27.5 and 28.5 MeV. Finally, the present data at the highest two energies, are in better agreement with Uno and the two evaluations than the previous data points. It is unclear at present why the data for this reaction are systematically high compared to the existing data and evaluations. The large uncertainty on the last data point comes primarily from the large correction for off-energy neutrons that is made to the flux and propagated into the cross-section value.

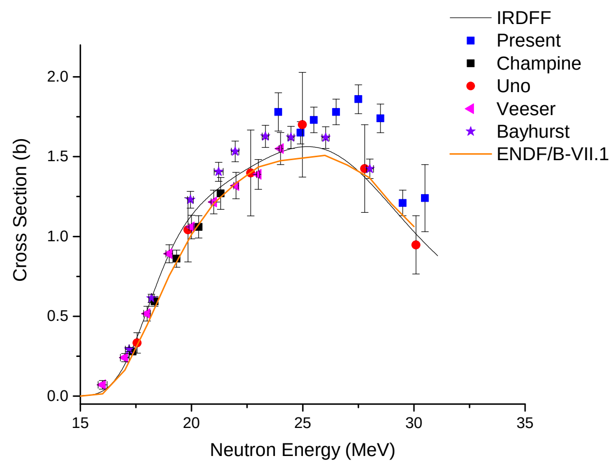

FIG. 7. (Color Online) Present data along with existing experimental data and evaluations for the ^{169}Tm(n,3n)^{167}Tm reaction.

TABLE V. Results from present measurements for the ^{169}Tm(n,3n)^{167}Tm reaction with quasi-monoenergetic neutrons. Uncertainties are given at the 1σ level.

Energy (MeV)	σ (b)
23.9 ± 0.105	1.78 ± 0.12
24.9 ± 0.130	1.65 ± 0.07
25.5 ± 0.133	1.73 ± 0.08
26.5 ± 0.138	1.78 ± 0.08
27.5 ± 0.142	1.86 ± 0.09
28.5 ± 0.147	1.74 ± 0.09
29.5 ± 0.156	1.21 ± 0.08
30.5 ± 0.165	1.24 ± 0.21

IV. CONCLUSION

The data presented above represents the most complete data set for the ^{209}Bi(n,4n)^{206}Bi reaction from threshold to 30 MeV. For the few data points that exist in this energy range there is good agreement. At present only calculated values of the ^{209}Bi(n,4n)^{206}Bi reaction cross-section have been used in the analysis of the Bismuth activation on the NIF. With the addition of this new cross-section data a much more accurate analysis of the Bismuth activation can be made resulting in improvements in the deduced charged-particle stopping power [2] that are determined using the Bismuth reaction. This is true especially below 26 MeV where the NIF RIF flux is largest and where the discrepancy between the current data and the evaluations is substantial.

The uncertainties in the presented data are dominated by the uncertainty in the reference cross-sections [10–12], which are between 5-12%. At these high incident neutron energies (i.e. above 20 MeV) the accuracy of the available reference cross-sections greatly decreases compared to lower-energies where there are significant number of measurements. Greater care is therefore needed in measuring the cross-sections of various reference reactions for incident neutron energies above 20 MeV.

V. ACKNOWLEDGEMENTS

We would like to thank the help of the TUNL Tandem support staff for maintaining the machine and providing needed assistance during the measurements. This work was supported by the National Nuclear Security Administration (NNSA) under contract no. DE-AC52-06NA25396.

[1] H. S. Park *et al.*, Physical Rev. Letters **112** (2014).
[2] A. C. Hayes *et al.*, Physics of Plasmas **22**, 082703 (2015).
[3] B. Champine, M. E. Gooden, Krishichayan, E. B. Norman, N. D. Scielzo, M. A. Stoyer, K. J. Thomas, A. P. Tonchev, W. Tornow, and B. S. Wang, Phys. Rev. **C 93**, 014611 (2016).
[4] J. Vrzalová, O. Svoboda, A. Krasá, A. Kugler, M. Majerle, and M. Suchopár, Nucl. Inst. and Meth. Phys. Res. Sect. A **726** (2013).
[5] E. Kim, T. Nakamura, A. Konno, Y. Uwamino, N. Nakanishi, M. Imamura, N. Nakao, S. Shibata, and S. Tanaka, Nuclear Science and Engineering **129**, 209 (1998).
[6] M. Drosg and N. Otuka, INDC(AUS)-0019 (2015).
[7] E. M. Zsolnay, R. Capote, H. K. Nolthenius, and A. Trkov, INDC(NDS)-0616 (2012).
[8] M. Chadwick *et al.*, Nuclear Data Sheets **112**, 2287 (2011).
[9] M. E. Gooden *et al.*, Nuclear Data Sheets **131**, 319 (2016).
[10] K. I. Zolotarev, INDC(NDS)-0546 (2009).
[11] K. I. Zolotarev, INDC(NDS)-0584 (2010).
[12] K. I. Zolotarev, INDC(NDS)-0657 (2013).
[13] A. Koning, D. Rochman, J. Kopecky, J. Ch. Sublet, E. Bauge, S. Hilaire, P. Romain, B. Morillon, H. Duarte, S. van der Mark, S. Pomp, H. Sjostrand, R. Forrest, H. Henriksson, O. Cabellos, S. Goriely, J. Leppanen, H. Leeb, A. Plompen, and R. Mills, *TENDL-2015: TALYS-based evaluated nuclear data library*, Tech. Rep. (`https://tendl.web.psi.ch/tendl_2015/tendl2015.html`).
[14] J.-C. Sublet, L. Packer, J. Kopecky, R. Forrest, A. Koning, and D. Rochman, *The European Activation File: EAF-2010 neutron induced cross section Library - CCFE-R (10) 05*.
[15] M. Zaman, G. Kim, K. Kim, H. Naik, M. Shadid, and M. Lee, European Physical Journal **A 51** (2015).
[16] M. Majerle, P. Bém, J. Novák, E. Šimečková, and M. Štefánik, Nuclear Physics **A 953** (2016).
[17] B. P. Bayhurst, J. S. Gilmore, R. J. Prestwood, J. B. Wilhelmy, N. Jarmie, B. H. Erkkila, and R. A. Hardekopf, Phys. Rev. **C 12** (1975).
[18] Y. Uno *et al.*, in *Proc. 9th International Symposium on Reactor Dosimetry, September 2-6, 1996, Prague, Czech Republic* (1998) pp. 465–472.